WHY COLOR CONSTANCY IMPROVES FOR MOVING OBJECTS

Marc Ebner
Ernst-Moritz-Arndt-Universität Greifswald, Institut für Mathematik und Informatik
Walther-Rathenau-Straße 47, 17487 Greifswald, Germany
Tel: (+49)3834/86-4646, Fax: (+49)3834/86-4640
marc.ebner@uni-greifswald.de

Keywords: Color constancy, color perception, computational modeling, object/scene motion

Abstract: Light which is measured by retinal receptors varies with the illuminant. However, a human observer is able to discount the illuminant and to accurately determine the color of objects. The human brain computes a color constant descriptor which is approximately independent of the illuminant. This ability is called color constancy. Recently, it has been shown that color constancy improves for a moving stimulus. It has been argued that high level motion areas may have an influence on the computation of a color constant descriptor. We have developed a computational model for color perception which can be mapped to the different stages of the human visual system. We test our model with two types of stimuli: stationary and moving. In our model, color constancy is computed purely bottom up. Our model also shows better color constancy for a moving stimulus. This indicates that an influence from high level motion areas is not required.

1 MOTIVATION

A human observer is able to perceive the color of objects as approximately color constant. This ability is know as Color Constancy (Zeki, 1993; Ebner, 2007a). Consider a scene with one or more light sources. The light is illuminating the objects of the scene. Some of the light is absorbed while the remaining light is reflected by the objects. Eventually, the light enters the eye where it is measured by the retinal receptors. The brain is able to compute a color constant descriptor from the light entering the eye even though this light varies with the color of the illuminant.

Suppose that an illuminant with a lot of energy in the red and green parts of the spectrum illuminates the scene. For such an illuminant, a digital sensor (with neutral white balance) will measure an image with a yellowish color cast. If the illuminant emits its light primarily in the blue part of the spectrum, then the digital image will have a bluish color cast. The problem of computing a color constant descriptor based only on data measured by the retinal receptors is actually underdetermined. Nevertheless, the brain somehow does arrive at a color constant descriptor which is independent of the illuminant. Cells found in V4 respond in a color constant way (Zeki and Marini, 1998; Zeki and Bartels, 1999). For instance, certain cells respond whenever a yellowish object enters the receptive field of this cell irrespective of the light which is actually reflected from the object.

Quite a number of computational algorithms have been proposed which address the problem of color constancy. Land (1974) has proposed the Retinex theory and together with McCann developed the first computational algorithm for color constancy (Land and McCann, 1971). The Retinex algorithm considers random paths running along an image created by a matrix of receptors with a logarithmic response. A color constant descriptor is computed by subtracting the data measured by adjacent receptors, applying a threshold function and then summing up the result. Extensions to the original Retinex algorithm have been proposed by Horn (1974) and Blake (1985). Moore et al. (1991) have implemented a version of the Retinex algorithm in hardware. Funt et al. (2004) give an implementation in Matlab.

Apart from the Retinex algorithm, several other algorithms have been proposed, e.g. the gray-world-assumption (Buchsbaum, 1980), recovery of basis-functions (Maloney and Wandell, 1986) or gamut-constraint methods (Forsyth, 1990). Most color constancy algorithms assume that the scene is uniformly illuminated. However, in practice multiple illuminants are present which cause a non-uniform illumination. For instance, some daylight may be falling through a window while an artificial illuminant may be switched on inside the room. Land and McCann's Retinex algorithm (Land and McCann, 1971) also works in the presence of a non-uniform illuminant.

Barnard et al. (1997) has extended the gamut constraint algorithm to scenes with non-uniform illumination. Neural architectures for color constancy have also been proposed (D'Zmura and Lennie, 1986; Dufort and Lumsden, 1991). As of now, it is not clear which algorithm is used by the brain to arrive at a color constant descriptor. Most computational algorithms for color constancy are quite complex and cannot readily be mapped to what is known about the human visual system. Ebner (2007b) has established a correspondence between his algorithm which is based on the computation of local space average color and the workings of the human visual system.

In a recent study, Werner (2007) has shown that, when an object moves, color constancy improves. Werner argues that high-level motion processing (attention driven) has an impact on color perception. With this contribution, we 1) extend Ebner's (2007a) color constancy model for color perception and 2) use this model to show how color constancy can improve if an object moves. This supports the hypothesis that Werner's results may be explained purely bottom up without the direct influence from high-level vision areas to color processing areas.

2 COLOR IMAGE FORMATION

In order to understand the computational model for color perception which is detailed in the next section, we first need a model of color image formation. Three types of cones can be distinguished (Dartnall et al., 1983). The retinal receptors respond to light in the red, green and blue parts of the spectrum (cones). We will use (x,y) coordinates to index the retinal receptors. The non-uniform spatial distribution of the receptors is of no concern in this context. Each receptor located at position (x,y) receives light from a corresponding object patch of the scene. Let $L(x,y,\lambda)$ be the irradiance falling onto the corresponding object patch for wavelength λ. Some of the irradiance is absorbed while the remainder is reflected into the surrounding. We assume that the objects are mainly diffuse reflectors, i.e. the incident light is reflected uniformly into the surrounding. The dichromatic reflectance model could be taken into account to model highlight reflections. However, they are usually localized and hence have a small impact on the model described here.

Let $R(x,y,\lambda)$ be the percentage of the reflected light at corresponding object position (x,y) and wavelength λ. Let $S_i(\lambda)$ be the sensitivity of cone $i \in \{r,g,b\}$ for wavelength λ. Then the energy $I_i(x,y)$ measured by retinal receptor i at position (x,y) can be modeled as (Ebner, 2007a)

$$I_i(,x,y) = G(x,y) \int S_i(\lambda) R(x,y,\lambda) L(x,y,\lambda) d\lambda. \quad (1)$$

where $G(x,y) = \cos(\alpha(x,y))$ is a geometry factor which depends on the scene geometry, i.e. the angle α between the normal vector and the direction to the light source at position (x,y). In case of an ideal receptor which responds only to a single wavelength λ_i, i.e. with $S_i(\lambda) = \delta(\lambda - \lambda_i)$, we obtain

$$I_i(,x,y) = G(x,y) R(x,y,\lambda_i) L(x,y,\lambda_i). \quad (2)$$

Thus, we see that the measured light at retinal position (x,y) is proportional to the reflectance R and the irradiance L. Let $\mathbf{I}(x,y) = [I_r(x,y), I_g(x,y), I_b(x,y)]$ be the measured light at retinal position, and $\mathbf{R}(x,y) = [R(x,y,\lambda_r), R(x,y,\lambda_g), R(x,y,\lambda_b)]$ be the reflectance and $\mathbf{L}(x,y) = [L(x,y,\lambda_r), L(x,y,\lambda_g), L(x,y,\lambda_b)]$ be the irradiance at the corresponding object point, then we write

$$\mathbf{I}(x,y) \propto \mathbf{R}(x,y) \cdot \mathbf{L}(x,y) \quad (3)$$

where $\cdot$ denotes component-wise multiplication. It is of course clear, that the retinal receptors are not narrow band. However, considering them as narrow band will allow us better to understand how the brain arrives at a color constant descriptor. Not having narrow band receptors complicates the performance of color constancy. Human color constancy correlates with reflectance estimation but is not perfect (McCann et al., 1976).

3 COMPUTATIONAL MODELING OF COLOR PERCEPTION

Ebner (2007b) has given a computational model of color constancy which estimates reflectance. It is based on the computation of local space average color (Ebner, 2009). Here, we provide an extended version of this model. The retinal receptors respond to the incoming light. Three types of receptors are modeled which absorb the light in the red, green and blue parts of the spectrum as described above. Let $\mathbf{c}$ be the energy measured by the receptors. All channels are scaled by the maximum value m with $m = \max_{i,x,y} I_i(x,y)$. This models the adaptation mechanism of the eye. We obtain

$$\mathbf{c}(x,y) = \frac{\mathbf{I}(x,y)}{m} \quad (4)$$

for the measured light $\mathbf{c}$ which also takes adaptation into account. The retinal cells also capture light from different directions as the eye or the stimulus moves. Let $\tilde{\mathbf{c}}$ be the output of this temporal averaging, i.e.

$$\tilde{\mathbf{c}}(x,y) = (1 - p_{t1}) \tilde{\mathbf{c}}(x,y) + p_{t1} \mathbf{c}(x,y) \quad (5)$$

with $p_{t1} = 0.8$.

The response of the retinal receptors can be modeled using either a logarithmic response curve as suggested by Faugeras (1979) or using a square root or cube root response curve as suggested by Hunt (1957). We will assume a cube root response function. The cube root response is also used for the CIE $L^*u^*v^*$ color space (International Commission on Illumination, 1996). All these different types of response curves can be used to approximate each other on a given range and with the right parameters (Ebner et al., 2007). Hence, the output of the retinal receptors $\mathbf{o}_\mathrm{r}$ is given by

$$\mathbf{o}_\mathrm{r} = \tilde{\mathbf{c}}^{1/3}. \tag{6}$$

The three retinal receptors create a three dimensional color space. Each measurement is represented by a point in this coordinate space. The color opponent and double opponent cells of V1 (Livingstone and Hubel, 1984; Tovée, 1996) transform this RGB color space to a rotated color space where the axes are dark-bright, red-green and blue-yellow. We do not incorporate this rotation of the color space into our computational model because the outcome is the same irrespective of the orientation of the coordinate system. Hence, we will omit this rotation here. Thus, we obtain for the signal processed in V1, $\mathbf{o}_{\mathrm{V1}} = \mathbf{o}_r$.

Cells found in V4 have been shown to respond in a color constant way (Zeki and Marini, 1998). Hence, we assume that the essential processing, which is required to compute a color constant descriptor, is located in V4. In our model, gap junctions between neurons in V4 create a resistive grid. Gap junctions are known to behave like resistors (Herault, 1996). The resistive grid is used to compute local space average color. Because of the resistive connection between adjacent neurons, some of the activation is exchanged between connected neurons. Let $N(x,y)$ be the set of neighboring neurons which are connected to a given neuron which processes information from retinal position (x,y). Thus, each neuron of the resistive grid computes local space average color $\mathbf{a}(x,y)$ iteratively using the update equations

$$\mathbf{a}'(x,y) := \frac{1}{|N(x,y)|} \sum_{(x',y') \in N(x,y)} \mathbf{a}(x',y') \tag{7}$$

$$\mathbf{a}(x,y) := \mathbf{o}_\mathrm{r}(x,y) \cdot p_a + \mathbf{a}'(x,y) \cdot (1 - p_a). \tag{8}$$

First, local space average color from neighboring neurons is averaged. The second step adds a little amount from the retinal input $\mathbf{o}_\mathrm{r}$ to the average which has been computed so far using a weighted average with the parameter p_a. The smaller the parameter p_a the larger the support over which local space average color is computed. For $p_a \to 0$, global space average color is computed. This is illustrated in Figure 1 where local space average color is computed using different values of p_a. For our experiment, we have used $p_a = 0.000758$. This value is chosen such that local space average color is computed over a sufficiently large area, e.g. 30% of the image. A color constant descriptor is computed in the next stage. Because this requires additional neural circuitry, the signal is again temporally averaged. Let $\tilde{\mathbf{a}}$ be the temporal average of local space average color, then $\tilde{\mathbf{a}}$ is computed using

$$\tilde{\mathbf{a}}(x,y) := p_{t2}\mathbf{a}(x,y) + (1 - p_{t2})\tilde{\mathbf{a}}(x,y) \tag{9}$$

with $p_{t2} = 0.1$.

In Ebner's (2007a) model, local space average color $\mathbf{a}$ is subtracted from the measured color $\mathbf{o}_\mathrm{r}$ to arrive at a color constant descriptor. Thus, we compute

$$\mathbf{o}_{\mathrm{V4}}(x,y) := \mathbf{o}_{\mathrm{V1}}(x,y) - \tilde{\mathbf{a}}(x,y). \tag{10}$$

The components of our model for color perception are illustrated in Figure 2. The color constant descriptor $\mathbf{o}_{\mathrm{V4}}$ has to be transformed before its data can be visualized using an RGB color space. In order to evaluate the performance of our computational model, we basically invert the pipeline as described above. In the coordinate space of the color constant descriptor, gray lies at the center of this space. First we have to apply a shift of the coordinate system followed by the inverse of the cube root function to obtain a reflectance estimate. The necessary shift can be computed by assuming a uniform distribution of colors. In this case, the shift is given as $\mathbf{d} = [k,k,k]$ with

$$k = \sum_{i=0}^{n} \left(\frac{i}{n}\right)^{\frac{1}{3}}. \tag{11}$$

The estimated reflectance $\tilde{\mathbf{R}}$ is then given as

$$\tilde{\mathbf{R}} = (|\mathbf{o}_{\mathrm{V4}} + \mathbf{d}|)^3. \tag{12}$$

4 COMPUTATION OF A COLOR CONSTANT DESCRIPTOR

The color constant descriptor is computed by subtracting local space average color $\mathbf{a}$ from the measured color $\mathbf{o}_{\mathrm{V1}}$ Ebner (2007b). Local space average color computed by a resistive grid can be approximated by the following function (Ebner, 2009)

$$\mathbf{a}(x,y) = k(x,y) \int\int_{x',y'} g(x-x', y-y')\mathbf{o}_{\mathrm{V1}} dx' dy' \tag{13}$$

where $g(x,y)$ is a smoothing kernel and $k(x,y)$ is a scaling factor with

$$k(x,y) = \frac{1}{\int\int_{x',y'} g(x-x', y-y') dx' dy'}. \tag{14}$$

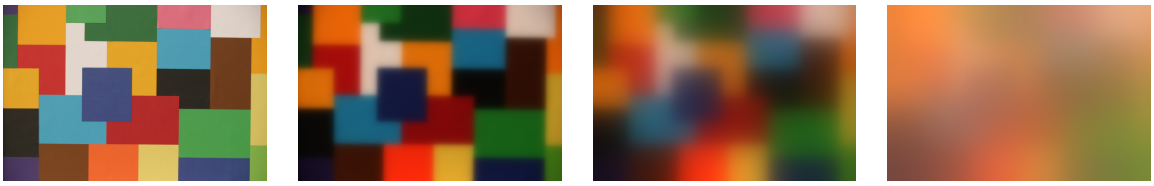

(a) (b) (c) (d)

Figure 1: (a) input image (size 614×410) (b-d) spatially averaged images (b) $p_a = 0.005$ (c) $p_a = 0.0002$ (d) $p_a = 0.00001$

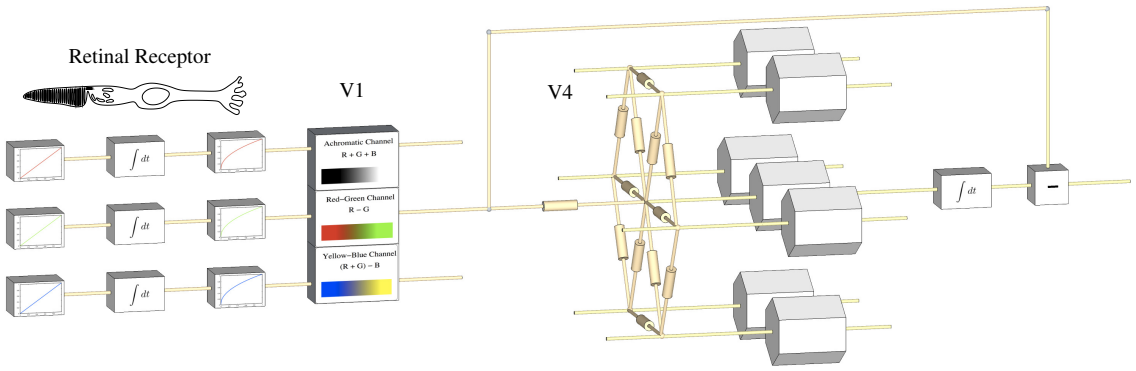

Figure 2: Computational model for color perception.

The smoothing kernel $g(x,y)$ can be approximated by the following function with smoothing parameter σ.

$$g(x,y) = e^{-\frac{|x|+|y|}{\sigma}} \tag{15}$$

The smoothing parameter depends on the parameter p_a with $\sigma = \frac{1-p_a}{4p_a}$. As we have described above, the response of the retinal receptors can be described by a cube root function or by a logarithmic function. Both functions are similar with a proper choice of parameters on the relevant data range. Using $\mathbf{o}_{V1} \propto \log(\mathbf{RL})$, we obtain a color constant descriptor $\mathbf{o}_{V1} - \mathbf{a}(x,y) = \log \mathbf{R}(x,y) - \text{constant}$. Note that in order to obtain this result, we have used the assumption that the illuminant varies slowly with respect to the support of the smoothing kernel, i.e. $\mathbf{L}(x,y)$ can be considered constant within the support. Similarly, it is assumed that several different reflectances are contained with in the area of support of the smoothing kernel.

5 EXPERIMENTS

Two types of stimuli are used in order to investigate the impact of motion on color constancy: A) stationary stimulus and B) moving stimulus. For stimulus A a stationary test patch is viewed in front of a stationary background. For stimulus B the same test patch moves across the background. The observer is assumed to fixate the test patch. These two stimuli

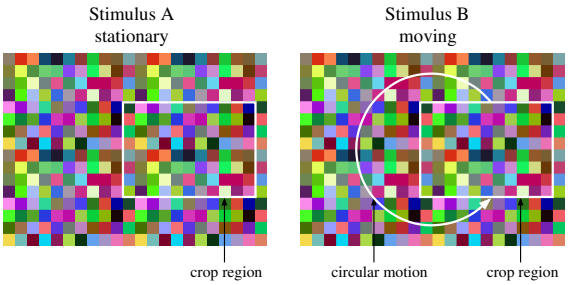

Figure 3: The stationary stimulus (A) is created by cropping a rectangular area from a larger random color checkerboard pattern. The moving stimulus (B) is created by moving the crop region along a circular path.

are evaluated with respect to the ability to compute a color constant descriptor.

The two stimuli originate from a random color checkerboard pattern as shown in Figure 3. For stimulus A, a smaller rectangular area is cropped from a larger checkerboard pattern. The test patch is overlaid in the center. The pattern stays stationary throughout the experiment. For stimulus B, the crop area moves in a circular motion across the background. Again, the test patch is displayed in the center of the crop area. All of the colors which have been used to generate the stimuli have been chosen at random.

Figure 4 shows the results for the two stimuli after 4320 iterations of the algorithm described in Section 3. The resistive grid of V4 is used to compute local

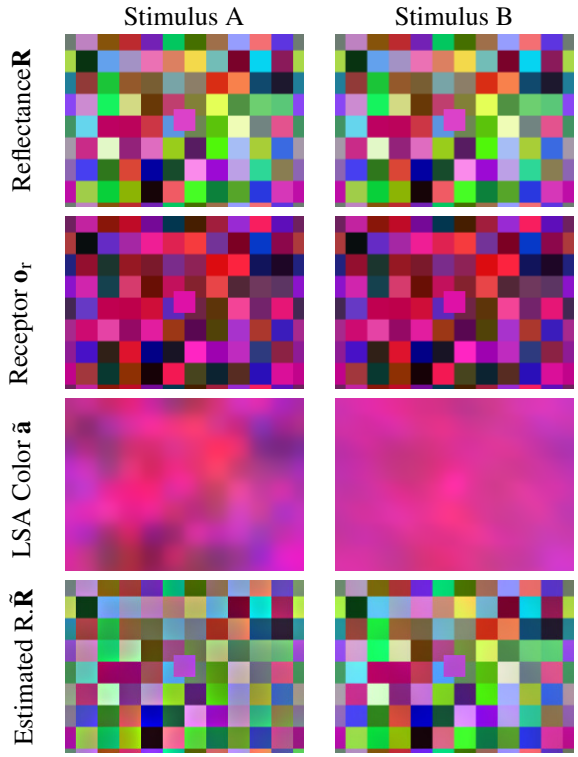

Figure 4: The first column shows the results when a static input stimulus is used. The second column shows the results when a moving stimulus is used. The first row of images shows the reflectance images $\mathbf{R}$. The second row shows the input stimulus $\mathbf{c}$. The third row shows the estimate of the illuminant, i.e. local space average color $\tilde{\mathbf{a}}$. The fourth row shows the internal color constant descriptor transformed back into RGB values $\tilde{\mathbf{R}}$. It is clear that the estimate of the illuminant improves greatly when the input stimulus moves.

space average color which is an estimate of the illuminant. It is clear that for stimulus B, local space average color $\tilde{\mathbf{a}}$ provides a much better estimate of the illuminant. This is because the background moves relative to the retinal receptors. Hence, local space average color is much smoother than for stimulus A. For a static stimulus, the retinal receptors are always exposed to the same input. Therefore, local space average color computed within one of the color patches is slightly biased towards the color of the patch. Figure 5 illustrates this bias for both stimuli. The bias image is computed by transforming local space average color back to RGB space and then dividing by the color of the illuminant.

We have repeated this experiment for 100 random starting positions of the crop region and also for 10 randomly chosen illuminants. In total 1000 experiments were performed. In order to evaluate the ability to compute a color constant descriptor, we compute the angular error $e(x,y)$ between the estimated reflectance $\tilde{\mathbf{R}}(x,y)$ and the actual reflectance $\mathbf{R}(x,y)$.

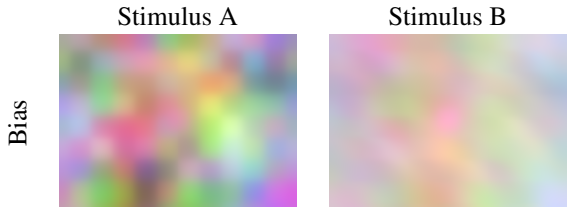

Figure 5: Bias due to the input stimulus. For stimulus A the bias is more pronounced. For stimulus B the estimate of local space average color is much better, hence the reflectance estimate is more accurate compared to stimulus A.

Table 1
Table 2: Average angular error $\bar{e}$ across all image pixels and all 1000 experiments.

	Angular Error $\bar{e}$	Std. Dev.
Stimulus A	6.0120	0.1507
Stimulus B	2.8283	0.1012

$$e(x,y) = \cos^{-1} \frac{\tilde{\mathbf{R}}(x,y)\mathbf{R}(x,y)}{|\tilde{\mathbf{R}}(x,y)||\mathbf{R}(x,y)|} \qquad (16)$$

Table 1 shows the average angular error $\bar{e}$ (average angular error over all image pixels and over all 1000 experiments) for the two stimuli A and B. The standard deviation is also shown. The angular error is significantly lower (t-test $t = 182.7$) when the background moves behind the test patch.

Werner (2007) has shown that motion improves the ability to correctly estimate the color of a given test patch. Werner argued that high-level motion processing may influence the computation of a color constant descriptor and that color processing and motion processing may not be completely separated. Here, we have given a computational model of color perception which shows the same behavior, i.e. color can be estimated better if the retinal receptors move across a background. In our model, color is computed bottom up. No high-level motion areas are simulated.

According to our view, motion processing does not have a direct impact on the computation of a color constant descriptor. Instead, motion processing is used to control the motion of the eye ball. If a test patch moves across a stationary background and the eye fixates the test patch, then the background moves behind the test patch in the same way that the background moved behind the test patch in our experiments. This causes the retinal receptors to be exposed to different inputs in the course of time. Because of the temporal integration, a more accurate estimate of the illuminant is obtained.

6 CONCLUSIONS

We have given a computational model for color perception. The retinal response is assumed to follow a cube root relationship. The first stage is adaptation followed by a temporal averaging process. By the time the visual stimulus has reached V1, a rotation of the coordinate system has occurred. In V4, local space average is computed through a resistive grid. This resistive grid is created by neurons which are laterally connected via gap-junctions. A color constant descriptor is computed by subtracting local space average color from the signal which is received from V1. Another temporal averaging occurs at the last stage. We have shown that this model is able to reproduce an important result from experimental psychology, namely that color constancy improves for a moving stimulus.

References

Barnard, K., Finlayson, G., and Funt, B. (1997). Color constancy for scenes with varying illumination. *Computer Vision and Image Understanding*, 65(2):311–321.

Blake, A. (1985). Boundary conditions for lightness computation in mondrian world. *Computer Vision, Graphics, and Image Processing*, 32:314–327.

Buchsbaum, G. (1980). A spatial processor model for object colour perception. *Journal of the Franklin Institute*, 310(1):337–350.

Dartnall, H. J. A., Bowmaker, J. K., and Mollon, J. D. (1983). Human visual pigments: microspectrophotometric results from the eyes of seven persons. *Proc. R. Soc. Lond. B*, 220:115–130.

Dufort, P. A. and Lumsden, C. J. (1991). Color categorization and color constancy in a neural network model of V4. *Biological Cybernetics*, 65:293–303.

D'Zmura, M. and Lennie, P. (1986). Mechanisms of color constancy. *Journal of the Optical Society of America A*, 3(10):1662–1672.

Ebner, M. (2007a). *Color Constancy*. John Wiley & Sons, England.

Ebner, M. (2007b). How does the brain arrive at a color constant descriptor? In Mele, F., Ramella, G., Santillo, S., and Ventriglia, F., eds., *Proc. of the 2nd Int. Symp. on Brain, Vision and Artificial Intelligence, Naples, Italy*, pp. 84–93, Berlin. Springer.

Ebner, M. (2009). Color constancy based on local space average color. *Machine Vision and Applications Journal*, 20(5):283–301.

Ebner, M., Tischler, G., and Albert, J. (2007). Integrating color constancy into JPEG2000. *IEEE Transactions on Image Processing*, 16(11):2697–2706.

Faugeras, O. D. (1979). Digital color image processing within the framework of a human visual model. *IEEE Trans. on*, ASSP-27(4):380–393.

Forsyth, D. A. (1990). A novel algorithm for color constancy. *Int. J. of Computer Vision*, 5(1):5–36.

Funt, B., Ciurea, F., and McCann, J. (2004). Retinex in MATLAB. *Journal of Electronic Imaging*, 13(1):48–57.

Herault, J. (1996). A model of colour processing in the retina of vertebrates: From photoreceptors to colour opposition and colour constancy phenomena. *Neurocomputing*, 12:113–129.

Horn, B. K. P. (1974). Determining lightness from an image. *Comp. Graphics and Image Processing*, 3:277–299.

Hunt, R. W. G. (1957). Light energy and brightness sensation. *Nature*, 179:1026–1027.

International Commission on Illumination (1996). Colorimetry, 2nd ed., Tech. Report 15.2.

Land, E. H. (1974). The retinex theory of colour vision. *Proc. Royal Inst. Great Britain*, 47:23–58.

Land, E. H. and McCann, J. J. (1971). Lightness and retinex theory. *J. of the Optical Society of America*, 61(1):1–11.

Livingstone, M. S. and Hubel, D. H. (1984). Anatomy and physiology of a color system in the primate visual cortex. *The Journal of Neuroscience*, 4(1):309–356.

Maloney, L. T. and Wandell, B. A. (1986). Color constancy: a method for recovering surface spectral reflectance. *J. of the Optical Society of America A*, 3(1):29–33.

McCann, J. J., McKee, S. P., and Taylor, T. H. (1976). Quantitative studies in retinex theory. *Vision Res.*, 16:445–458.

Moore, A., Allman, J., and Goodman, R. M. (1991). A real-time neural system for color constancy. *IEEE Transactions on Neural Networks*, 2(2):237–247.

Tovée, M. J. (1996). *An introduction to the visual system*. Cambridge University Press, Cambridge.

Werner, A. (2007). Color constancy improves, when an object moves: High-level motion influences color perception. *Journal of Vision*, 7(14):1–14.

Zeki, S. (1993). *A Vision of the Brain*. Blackwell Science, Oxford.

Zeki, S. and Bartels, A. (1999). The clinical and functional measurement of cortical (in)activity in the visual brain, with special reference to the two subdivisions (V4 and V4α) of the human colour centre. *Proc. R. Soc. Lond. B*, 354:1371–1382.

Zeki, S. and Marini, L. (1998). Three cortical stages of colour processing in the human brain. *Brain*, 121:1669–1685.